HHS Public Access

Author manuscript

Magn Reson Med. Author manuscript; available in PMC 2018 September 01.

Published in final edited form as:

Magn Reson Med. 2017 September ; 78(3): 909–916. doi:10.1002/mrm.26471.

3D in utero quantification of T2* relaxation times in human fetal brain tissues for age optimized structural and functional MRI

Anna I Blazejewska[a], **Sharmishtaa Seshamani**[a], **Susan K McKown**[b], **Jason S Caucutt**[c], **Manjiri Dighe**[b], **Christopher Gatenby**[b], and **Colin Studholme**[a,d]

[a]Department of Pediatrics, University of Washington

[b]Department of Radiology, University of Washington

[c]Institute of Translational Health Sciences, University of Washington

[d]Department of Bioengineering, University of Washington

Abstract

Purpose—Maximization of the BOLD fMRI contrast requires TE of the MR sequence to match the T2* value of the tissue of interest, which is expected to be higher in the fetal brain compared to a child or an adult.

Methods—T2* values of the cortical plate/cortical grey matter tissue in utero in healthy fetuses from mid-gestation onwards (20–36 GW) were measured using 3D T2* maps calculated from 2D dual-echo T2*-w data corrected for between-slice motion and reconstructed in 1.0 mm^3 isotropic resolution from a sequence of multiple time points, together with 1.0 mm^3 isotropic resolution T2-w structural data.

Results—Mean T2* relaxation times of the cortical tissue were about two times higher than previously reported in adults. In a supporting single seed analysis experiment default mode and auditory networks appeared better localized and less noisy while using TE=100 ms versus TE=43 ms. The results of the previous study reporting a trend for T2* values to decrease with fetal age were reproduced and extended to include subjects in earlier gestation (20–26 GW) and cortical tissues.

Conclusions—The first measurement of T2* values in fetal cortical tissues suggested the appropriate TE range for fetal BOLD fMRI protocol optimization to be 130–190 ms.

Keywords

fetal MRI; fMRI; in utero T2* relaxometry; brain development; MR tissue properties; fMRI sequence optimization

Corresponding Author: Anna Blazejewska, ania.blazejewska@gmail.com, BICG, Department of Pediatrics, Division of Neonatology, University of Washington, 1959 NE Pacific St, HSC RR447, Box 356320, Seattle, WA 98195, phone: 206 221 3002, fax: 206 543 8926.

Introduction

The human brain development taking place in utero during gestation and continuing into the neonatal period consists of a series of complex anatomical and physiological events. The process involves the growth and migration of the cells, synaptogenesis and myelination, and results in changes of measureable tissue properties within different anatomical regions. Importantly, tissue characteristics of a developing brain can differ significantly when compared with those observed in the brain of a healthy adult or a child, including increased levels of water content, lower macromolecular concentration and reduced synaptic density. All of these can influence the transverse and longitudinal MR relaxation times of the tissues and therefore may be open to investigation using non-invasive MRI techniques. A better understanding of the tissue relaxation values in-utero could potentially help to explain the nature of these measures and provide useful markers for the clinical evaluation of brain abnormalities in utero.

Elevated T2* relaxation times have been recently reported in prematurely born infant brains as compared to adults, including regions of white matter (WM) and deep gray matter, such as the Thalamus (THA) (1,2). Previous research conducted in human fetuses in utero reported T1 values in WM (3) and T2* values in various regions of WM and in the THA (4) to be significantly higher than those measured in the adult brain, with a trend to decrease with fetal age found for the T2* values.

Interest in the possibility of fetal brain fMRI has increased recently (5–13), motivated by the need of better understanding of the functional development of a human brain at its early stages, as well as by a potential clinical impact of the findings allowing for early diagnosis of certain diseases or abnormalities. The accurate assessment of T2* relaxation times in the fetal brain is important for the maximization of the blood oxygen level dependent (BOLD) contrast in the fMRI experiments, which requires the TE of the MRI sequence to match the T2* value of the tissue of interest (14). The standard protocols currently applied to study fetal and infant brain fMRI have simply used acquisition parameters optimized for adult subjects. Therefore, it is crucial to investigate T2* values of different tissue zones of the fetal brain, especially the cortical gray matter/cortical plate (CGM/CP), at different stages of development, in order to correctly optimize fMRI BOLD protocols. To the best of our knowledge, there is no existing study investigating T2* values in the cortical and subplate (SUB) tissue of the fetal brain in utero.

One of the main difficulties in fetal imaging in utero is motion, which cannot be controlled or tracked during the scanning process. In order to accurately assess relaxation parameters of different types of tissue in the fetal brain, high quality MR images are necessary. This requires employing motion estimation algorithms allowing post-hoc correction of the extensive between-slice fetal motion and 3D reconstruction. In order to distinguish thin layers of the cortical tissue in the small fetal brain high image resolution is also essential. The only existing study investigating T2* values in fetuses used slice-based 2D multi-echo approach which minimized the between-echo interval (4). However, this method did not deal with the between-slice motion problem and therefore did not allow 3D reconstruction of the whole brain volume for 3D examination of the brain tissue properties.

In the first part of this study, we investigated for the first time CGM/CP T2* values of the fetal brain in utero using motion corrected dual-echo 3D reconstructions and a high resolution conventional T2-w structural data. We used dual-echo multi-slice EPI acquisition, where between-slice motion was corrected and repeated time frames were combined to increase the signal, allowing 3D mapping of T2* values in the presence of fetal head motion. We applied this method to a cohort of healthy fetuses from mid-gestation onwards extending previously published measurements (4) into the 20–26W period, where many clinical MRIs are acquired after an earlier ultra-sound evaluation of pregnancy. As the second part of this work, we performed a preliminary single seed analysis experiment limited to two subjects looking into default mode and auditory networks in order to compare standard and longer echo times in fMRI experiments in utero.

Methods

In the first part of our study fifteen scanning sessions of healthy fetuses in the age range 20–36 gestational weeks (GW), female/male/unknown 6/5/2, mothers' age 32±3 Y, were performed including two re-scan sessions of the same subjects 5 and 9 weeks later. The second part included two fetuses in 29 and 32 GW, one male and one female, mothers' ages 29 and 28 Y, respectively. Written informed consent to undergo MRI was obtained from all participants and the study protocol was approved by the Institutional Review Board (IRB) of University of Washington. Acquired MRI datasets were post hoc evaluated by a radiologist to confirm absence of any pathological changes in the fetuses included in the study.

All the data were acquired using a 1.5T Philips Achieva scanner equipped with a 16 channel "Torso XL" coil. For both parts of the study the scanning protocol consisted of T2*-w 2D EPI dual-echo acquisition with TE1=15 ms, TE2≈43 ms TR=3000 ms, spatial resolution 3.0×3.0 mm^2, 3.0 mm slice thickness, 24–32 slices, 90–150 time points, interleave equal to a square root of number of slices (Philips default), one package, acquisition time ≈6 min. Both phase and magnitude images were acquired. TE1 was set to the shortest possible value to allow accurate unwrapping of the phase data, TE2 was based on typical values used in fMRI of adult brain. In the second part of this study an additional T2*-w EPI acquisition was acquired which differed only in second echo time TE2=100 ms. Each scanning session included three T2-w 2D HASTE scans acquired in 3 approximately orthogonal planes (sagittal, coronal, axial) consisting of 3–4 stacks each with spatial resolution 1.0×1.0 mm^2, 3.0 mm slice thickness, TE/TR=150–250/1000–3000 ms, 22–36 slices, interleave equal to a square root of number of slices, acquisition time ≈5 min.

1. T2* mapping of the tissues

Each of two EPI images of a dual-echo fMRI acquisition was processed separately following the procedure described below. First, correction of the susceptibility distortions that can arise from air spaces in the maternal digestive system was performed. The applied method used unwrapped phase data acquired with two different echo times to create a field map and generate a voxel shift map at each time point of the acquisition (15). Second, for each fMRI dataset all time points were automatically aligned to a manually repositioned reference frame (usually corresponding to the 1st time point) and transformed from the scanner

acquisition coordinates into a standard coordinate frame using the SLice MRI Motion Estimation and Reconstruction (SLIMMER) tool (16). The brain masks used by SLIMMER were based on manually delineated fetal brain segmentations averaged for subjects within age ranges of 2 GW in order to represent the appropriate brain size and shape. Finally, to correct the effects of fetal head motion that occurred between the acquisitions of subsequent slices (between-slice motion), cascaded slice to volume registration was applied (17). The final 3D T2*-w reconstructions were created in 1.0 mm^3 isotropic resolution by applying linear interpolation at the initialization step followed by the iterative optimization process. Combining volumes acquired at multiple time points into one 3D reconstruction allowed using the information about multiple views of the same anatomy of the moving fetal brain for resolving some of the errors caused by the partial volume effect. In addition, the slices affected by spin history effects are treated as outliers by this algorithm and their positions are estimated from the slices acquired at neighboringtimes. Upsampling of the data was motivated by the aim of measuring T2* values in the cortical tissue of the fetal brain which, especially in younger fetuses, may not exceed 1.0 mm in thickness. T2* maps were calculated voxel wise from the 3D reconstructions of both echo images for each acquisition. This final part of the processing scheme is illustrated in Figure 1.

Conventional T2-w data acquired with high in plane resolution (1.0×1.0 mm^2) and 3.0 mm slice thickness in three approximately orthogonal planes of the subject coordinate system were loaded into the SLIMMER tool and transformation into a standard coordinate frame was calculated for each of the stacks. Between-slice motion was estimated using the slice intersection motion correction SIMC approach, which simultaneously co-aligns multiple stacks of 2D slices using a matching structure along intersecting slice pairs acquired in orthogonal planes (18). A 3D reconstruction based on iterative deconvolution was performed to obtain a final high resolution isotropic (1.0 × 1.0 × 1.0 mm^3) volumes from the motion scattered slices (19). These images were subsequently mapped to the voxel coordinate system of the final 3D T2*-w reconstructions using a rigid body transformation.

Manual segmentation of the regions of interest (ROI) was carried out using the rview software (http://rview.colin-studholme.net). Different tissue types were delineated on transformed T2-w images viewed together with the corresponding T2* maps. The CGM (fetus age >25 GW) or CP (fetus age <25 GW)) ROIs were outlined on the sagittal slices and corrected in the coronal view to minimize partial volume effect (with WM/SUB or CSF), choosing cortical tissue in the most prominent sulci in older fetuses and cortical tissue adjacent to the inter-hemispheric fissure in younger fetuses (Figure 2). The THA ROIs were segmented in the axial plane and the frontal lobe WM (FWM) ROIs were segmented in the sagittal plane in the eleven oldest subjects in age range 26–37 GW (Figure 2). In the three youngest subjects, age 20–23 GW, different tissue layers within the region corresponding to the frontal lobe were still visible in T2-w images. Therefore, two separate ROIs were used to distinguish SUB tissue hyperintense in T2-w from the remaining hypointense part of the lobe corresponding to the intermediate zone (IZ) and subventricular/ventricular zone (VZ) (Figure 2). Mean T2* values were calculated within ROIs for all the maps and plotted against subjects' age.

2. Single seed analysis

As a second part of the study, single seed analysis of fMRI data acquired with two different TEs was performed on two fetal subjects. The initial processing of both EPI datasets, with TE2=43 ms and TE2=100 ms, included the same stages as performed in the first part of the study. Subsequently, cascaded slice to volume registration was then applied to each fMRI acquisition in order to correct for between-slice head motion and reconstruct sequences of T2*-w images in original 3.0 mm^3 isotropic resolution across all the time points. For each subject two multi-frame R2* maps were created using voxel wise least square regression, one for each TE2.

T2-w high resolution images were reconstructed from multiple stacks with the method described in the first part of the study and used to outline the seeds for default mode network (DMN) and auditory network (AN). The seeds were created applying 3D dilation to grow a manually selected voxel placed in praecuneus for DMN and in both sides of the auditory cortex separately for left and right AN, until the seed included 60–80 voxels (0.06–0.08cm^3), depending on the size of the brain. Binary seed masks were transformed to the space of R2* maps using linear interpolation (with the intensity threshold 0.5) and single seed analysis were performed using in house developed software. The final results were presented overlapped with the structural images. In addition, the values of the percentage of brain voxels presenting a correlation above the threshold of 400 were calculated for all the seeds. T2* values within WM, cGM and THA ROIs were measured using maps created for both pairs of TEs.

Results

1. T2* mapping of the tissues

Parameters of the fetal head motion estimated in reference to the volume acquired in the first time point (in a relation to the center of the image) from the slice transformations of T2*-w data time series, averaged across all the subjects, time points and slices, were: −0.3±1.4, 1.7±5.0, −1.0±3.3 mm of translation along x, y, z axes, 3.0±10.8, 1.9±4.2 and 1.9±3.2 degree of rotation in relation to the x, y, z, axes. Figure 3 presents motion plots illustrating translation and rotation of a fetus measured between the consecutive slices (as acquired in time) of the imaging sequence plotted for a subject (22GW) presenting an average amount of motion.

Volumes of the ROIs plotted against the subjects' age showed an increasing trend consistent with the subjects' age, except for SUB, which was gradually disappearing in older fetuses (Figure 4). This was expected based on the knowledge about the development of brain tissue and validated the process of ROIs selection. R-squared values calculated for the trends were 0.79, 0.84, 0.74, 0.87 and 0.93 for CGM/CP, THA, FWM, SUB and IV/VZ, respectively.

Mean T2* values calculated for all the ROIs were plotted against the subjects' age in Figure 5 with error bars in corresponding to the standard deviations of the T2* values within the ROI. Significant correlations were found between decreasing T2* values and increasing fetal age for CGM/CP ($p<0.0001$), THA ($p<0.0001$) and FWM ($p<0.01$), while values for SUB and IV/VZ in four analyzed subjects between 20–23 GW were relatively constant.

Interestingly, values obtained for these two ROIs were lower than calculated for FMW in older fetuses (Figure 5). Average value of a standard deviation as a percentage of the mean calculated for all the subjects was 22%, 14%, 20%, 23% and fell into range of 18–29%, 8–28%, 13–27%, 17–25% for CGM/CP, THA, FWM or IV/VZ and SUB, respectively.

Table 1 summarizes mean values of T2* measured in all investigated tissues averaged across all subjects and compares our results with these previously reported in the literature for fetuses, pre-mature newborns, infants and adults. R-squared values for CGM/CP, THA and FWM were high, reaching 0.68, 0.68 and 0.59, and low for IZ/VZ and SUB, 0.08 and 0.15, respectively.

2. Single seed analysis

The correlation maps calculated for two subjects and for all three seeds are presented in Figure 6 overlaid on the structural data. Comparison of the maps obtained from the datasets including images acquired with 43 ms and 100 ms echo times showed DMN, left and right AN to be better localized and less noisy in cases with TE=100 ms. This finding was confirmed by the decreased percentage of brain voxels presenting a correlation above a given threshold of 400 in maps acquired for longer TE, except for ANL in subject 2, where results for both TEs were comparable (Table 2). AN correlation maps did not show high values within the appropriate region on the side opposite to the seed ROI in all the cases.

T2* values calculated using two echo pairs (with longer TE of 43/100 ms, respectively), for two subjects (29 and 32 GW, respectively) were 167/168 ms and 143/136 ms for cGM, 174/174 ms and 155/140 ms for THA, and 285/303 ms and 220/194 ms for WM.

Discussion

We presented the first report of the T2* relaxation values measured in cortical tissues of the fetal brain in utero using 3D T2* maps created by applying between-slice motion correction and high resolution image reconstruction using a sequence of multiple time points to provide robust estimates. The mean T2* value calculated across all the subjects (163ms, Table I) was about two times higher than previously reported for adults using the same field strength (84ms, Table I) (20) and correlated with increasing fetal age (Figure 4). This difference should be taken into account when optimizing the TE values for BOLD fMRI sequences applied in fetal brain imaging, which currently uses similar parameters as adult studies. This preliminary result suggests that, depending on the actual age of the scanned fetal subject, TE values for BOLD fMRI at 1.5T should be chosen from the range of 130–190ms (corresponding approximately to mean ± standard deviation reported for the cortical tissues for subjects 20–36GW), however further research is necessary to provide recommendations regarding specific age groups. It has to be taken into account that long TE optimized to maximize BOLD signal may not necessarily be the best choice from the data quality point of view leading to increased signal loss, more severe spin history effects and motion related artifacts.

The developmental trend reported for the T2* values to be higher in younger fetuses (4), was confirmed in FWM/IZ/VZ and THA, with significant correlations between T2* values and

fetal age found for FWM and THA. Importantly, as a novel finding of this study, we observed a similar trend and significant correlation for CGM/CP, which is especially important for the BOLD fMRI studies. In addition, the results obtained for the healthy subjects in the previous study that focused on WM and THA (4) were extended here to include earlier gestation (20–26GW), which is potentially more relevant for many clinical studies. The trend for T2* to continue decreasing with age during later stages of brain development, is consistent with the results obtained in earlier studies of babies aged 9 months (1) and in adults (1,20).

Mean T2* values calculated within FWM/IZ/VZ and THA were similar, but slightly higher than those previously measured in healthy fetuses in late gestation (4), which would be expected considering the lower average age of the subjects in our study (29 vs 32 GW). There was an agreement between the results we obtained for THA and those reported by the previous studies in premature newborns of the similar age (1), however our results for FWM/IZ/VZ were much higher (Table I). Interestingly mean T2* values calculated for SUB and IZ/VZ regions tended to be lower than FWM relaxation times in older ages (Figure 5), but low R-squared values obtained for these tissues suggest that the results are not conclusive and require reinvestigation using a larger number of subjects.

To date only one previous T2* study has been performed on the human fetal brain in-utero, showing the feasibility of slice-based multi-echo T2* measurements (4). The technique employed in this early study acquired multiple echoes at each slice location before proceeding to imaging the next slice location. Such an approach minimizes motion between the subsequent echoes, but makes it less feasible to recover between-slice motion in order to reconstruct a 3D volume because of the time between spatially neighboring slices.

In this work, we used a novel approach allowing 3D T2* brain mapping, based on dual-echo multi-slice acquisition where between-slice motion was estimated and corrected. It has previously been shown that T2* values within WM regions measured in utero using one dual-echo acquisition are comparable to these calculated based on five T2*-w images acquired with different echo times (21). The final 3D T2*-w reconstructions were created in 1.0 mm^3 isotropic resolution using all acquired time points, in order to increase the signal-to-noise ratio of the T2* maps and also average out the possible contribution of a BOLD effect. In addition, T2* (R2*) maps have been previously shown to allow more reliable functional signal extraction (22) and to be less prone to bias and spin history effects compared to T2*-w images in case of a severe subject motion (12). Between-slice motion correction, 3D reconstruction, and high resolution of the final T2* maps allowed us to perform first measurements of the T2* values of cortical tissues in utero.

Preliminary experiment performing single seed analysis using R2* maps obtained from datasets acquired with two different echo times, shorter (43ms) and longer (100ms) demonstrated better localization of DMN, left and right AN in the correlation maps calculated for longer TE. Lack of strong correlations between both sides of AN in all of the analyzed cases was expected for the subjects in this age range (29 and 32GW) (23). The T2* values measured from the T2* maps calculated for both TE2s were comparable and consistent with the previous result based on fetal age for all three tissue types.

There were several limitations to this study. The assumption that the optimal BOLD contrast is acquired with TE of the sequence matching T2* of the cortex is only valid in the thermal noise domination regime (14). Several factors such as voxel size or subject motion may increase a contribution of physiological noise (24), therefore this assumption may be questionable in fetal imaging.

The echo time of 100 ms used in the experiment performing single seed analysis on two fetal subjects remained below the expected T2* values of the fetal cortical tissue. This was determined by the practical reasons of keeping the total scan time within the limits feasible for the subjects in their special condition, as well as by an expected signal loss and increased motion related artifacts with longer TE. In addition, due to the limited number of subjects used in single seed analysis experiment, these results can only be treated as preliminary, showing possible direction for the future studies.

Finally, a relatively small number of fetuses in mid-gestation (<26GW) available for analysis caused SUB T2* measurements to remain inconclusive. Further work will also include improving image reconstruction techniques, especially applying a newly developed robust method for 4D T2* mapping (12). In addition, more experiments examining T2* values obtained from the acquisitions with long echo times is required to support TE recommendations for the specific fetal age groups.

Conclusions

To the best of our knowledge this is the first measurement of T2* relaxation times in the cortical tissues of the fetal brain in utero. We showed a trend for the T2* values to decrease with the fetal age, including healthy fetuses from age range down to 20GW, which is critical for optimizing sequence parameters (TE values) of the protocols used in fetal BOLD fMRI. This study included first 3D maps of T2* relaxation values revealing age related decrease of the T2* measurements in frontal WM, THA and the most importantly cortical tissues of the fetal brain.

Acknowledgments

This work was funded by NIH grants R01 EB017133, R01 NS055064, UL1TR000423 and University of Washington internal funds.

References

1. Rivkin MJ, Wolraich D, Als H, McAnulty G, Butler S, Conneman N, Fischer C, Vajapeyam S, Robertson RL, Mulkern RV. Prolonged T*2 values in newborn versus adult brain: Implications for fMRI studies of newborns. Magn Reson Med. 2004; 51:1287–91. DOI: 10.1002/mrm.20098 [PubMed: 15170852]
2. Lee J, Shmueli K, Kang B-T, Yao B, Fukanaga M, van Gelderen P, Palumbo S, Bosetti F, Silva AC, Duyn JH. The contribution of myelin to magnetic susceptibility-weighted contrasts in high-field MRI of the brain. NeuroImage. 2012; 59:3967–3975. [PubMed: 22056461]
3. Abd Almajeed A, Adamsbaum C, Langevin F. Myelin characterization of fetal brain with mono-point estimated T1-maps. Magn Reson Imaging. 2004; 22:565–72. DOI: 10.1016/j.mri.2004.01.004 [PubMed: 15120177]

4. Vasylechko S, Malamateniou C, Nunes RG, Fox M, Allsop J, Rutherford M, Rueckert D, Hajnal JV. T2* relaxometry of fetal brain at 1.5 Tesla using a motion tolerant method. Magn Reson Med. 2014; 00doi: 10.1002/mrm.25299
5. Jardri R, Pins D, Houfflin-Debarge V, Chaffiotte C, Rocourt N, Pruvo J-P, Steinling M, Delion P, Thomas P. Fetal cortical activation to sound at 33 weeks of gestation: a functional MRI study. NeuroImage. 2008; 42:10–8. DOI: 10.1016/j.neuroimage.2008.04.247 [PubMed: 18539048]
6. Fulford J, Gowland PA. The emerging role of functional MRI for evaluating fetal brain activity. Semin Perinatol. 2009; 33:281–8. DOI: 10.1053/j.semperi.2009.04.006 [PubMed: 19631088]
7. Schöpf V, Kasprian G, Brugger PC, Prayer D. Watching the fetal brain at “rest”. Int J Dev Neurosci. 2012; 30:11–7. DOI: 10.1016/j.ijdevneu.2011.10.006 [PubMed: 22044604]
8. Jakab A, Schwartz E, Kasprian G, Gruber GM, Prayer D, Schöpf V, Langs G. Fetal functional imaging portrays heterogeneous development of emerging human brain networks. Front Hum Neurosci. 2014; 8:1–17. DOI: 10.3389/fnhum.2014.00852 [PubMed: 24474914]
9. Schöpf V, Schlegl T, Jakab A, Kasprian G, Woitek R, Prayer D, Langs G. The relationship between eye movement and vision develops before birth. Front Hum Neurosci. 2014; 8:775.doi: 10.3389/fnhum.2014.00775 [PubMed: 25324764]
10. Thomason ME, Dassanayake MT, Shen S, et al. Cross-hemispheric functional connectivity in the human fetal brain. Sci Transl Med. 2013; 5:173ra24.doi: 10.1126/scitranslmed.3004978
11. Ferrazzi G, Kuklisova Murgasova M, Arichi T, et al. Resting State fMRI in the moving fetus: a robust framework for motion, bias field and spin history correction. NeuroImage. 2014; 101:555–68. DOI: 10.1016/j.neuroimage.2014.06.074 [PubMed: 25008959]
12. Seshamani S, Blazejewska A, Gatenby C, Mckown S, Caucutt J, Dighe M, Studholme C. Robust R2* Map Estimation from Motion Scattered Slices for Fetal fMRI. IEEE Intl Symposium on Biomedical Imaging. 2015:2–5.
13. Seshamani S, Cheng X, Fogtmann M, Thomason ME, Studholme C. A Method for handling intensity inhomogenieties in fMRI sequences of moving anatomy of the early developing brain. Med Image Anal. 2014; 18:285–300. DOI: 10.1016/j.media.2013.10.011 [PubMed: 24317121]
14. Bandettini PA, Wong EC, Jesmanowicz A, Hinks RS, Hyde JS. Spin-echo and gradient-echo EPI of human brain activation using BOLD contrast: a comparative study at 1.5 T. NMR Biomed. 1994; 7:12–20. DOI: 10.1002/nbm.1940070104 [PubMed: 8068520]
15. Hutton C, Bork A, Josephs O, Deichmann R, Ashburner J, Turner R. Image distortion correction in fMRI: A quantitative evaluation. NeuroImage. 2002; 16:217–40. DOI: 10.1006/nimg.2001.1054 [PubMed: 11969330]
16. Kim, K., Habas, PA., Rajagopalan, V., Scott, J., Rousseau, F., Barkovich, AJ., Glenn, OA., Studholme, C. SLIMMER: SLIce MRI motion estimation and reconstruction tool for studies of fetal anatomy. In: Dawant, BM., Haynor, DR., editors. SPIE Medical Imaging. International Society for Optics and Photonics; 2011. p. 79624D
17. Seshamani S, Fogtmann M, Cheng X, Thomason M, Gatenby C, Studholme C. Cascaded Slice to Volume Registration for Moving Fetal fMRI. IEEE 10th International Symposium on Biomedical Imaging. 2013:796–799.
18. Kim K, Habas PA, Rousseau F, Glenn OA, Barkovich AJ, Studholme C. Intersection based motion correction of multislice MRI for 3-D in utero fetal brain image formation. IEEE Trans Med Imaging. 2010; 29:146–158. DOI: 10.1109/TMI.2009.2030679 [PubMed: 19744911]
19. Fogtmann M, Studholme C. A unified approach for motion estimation and super resolution reconstruction from structural Magnetic Resonance imaging on moving subjects. MICCAI workshop. 2012:9–16.
20. Peters AM, Brookes MJ, Hoogenraad FG, Gowland PA, Francis ST, Morris PG, Bowtell R. T2* measurements in human brain at 1.5, 3 and 7 T. Magn Reson Imaging. 2007; 25:748–53. DOI: 10.1016/j.mri.2007.02.014 [PubMed: 17459640]
21. Blazejewska AI, Seshamani S, Mckown S, Caucutt J, Dighe M, Gatenby C, Studholme C. Full 3D mapping of T2* relaxation times from mid to late gestation of the normal fetal brain. Intl Soc Mag Reson Med. 2015; 23:0644.

22. Seshamani S, Gatenby C, Fogtmann M, Cheng X, Dighe M, Studholme C. Combining R2* Mapping and Slice Registration for fMRI Analysis of Moving Subjects. Intl Soc Mag Reson Med. 2013; 21:3351.

23. Doria V, Beckmann CF, Arichi T, et al. Emergence of resting state networks in the preterm human brain. Proc Natl Acad Sci. 2010; 107:20015–20020. DOI: 10.1073/pnas.1007921107 [PubMed: 21041625]

24. Hyde JS, Biswal BB, Jesmanowicz A. High-resolution fMRI using multislice partial k-space GR-EPI with cubic voxels. Magn Reson Med. 2001; 46:114–125. DOI: 10.1002/mrm.1166 [PubMed: 11443717]

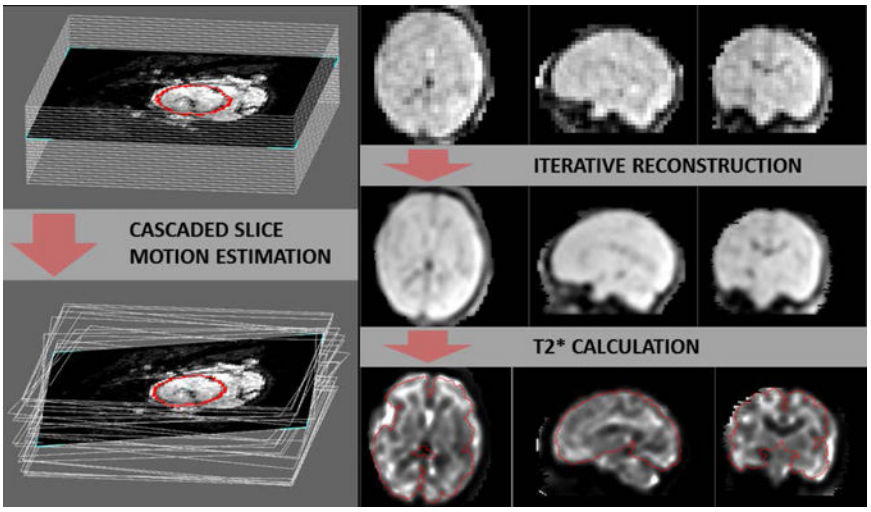

Figure 1.

Left: Illustration of the between-slice motion correction process using cascaded slice motion estimation: example stack of slices before (top) and after correction (bottom). Right: Three stages of data processing presented on an example dataset, one frame of T2*-w sequence acquired with the longer TE after volume registration (top row), iterative reconstruction of the high resolution (1mm isotropic) T2*-w image from all time frames (middle row) and subsequently calculated R2* map (bottom row). Brain has been outlined in red.

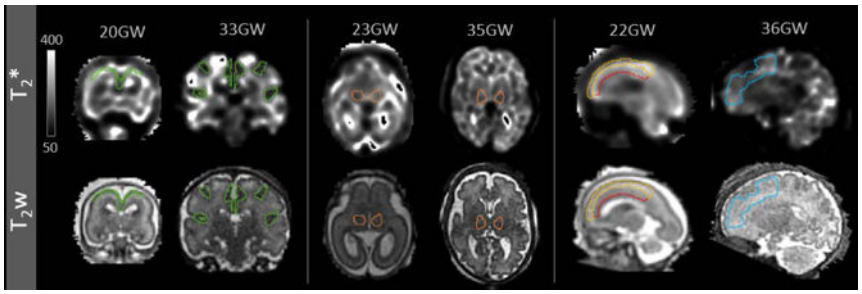

Figure 2.

The outlines of ROIs presented on slices of T2* maps and T2w images used for drawing; CGM/CP (left, green) and THA (middle, orange), for younger (20 and 23 GW) and older (33 and 35GW) subjects; SUB (yellow) and the remaining part of the frontal lobe (IZ/VZ, red) in a young subject (22GW, left) and FWM in an older subject (36GW, right).

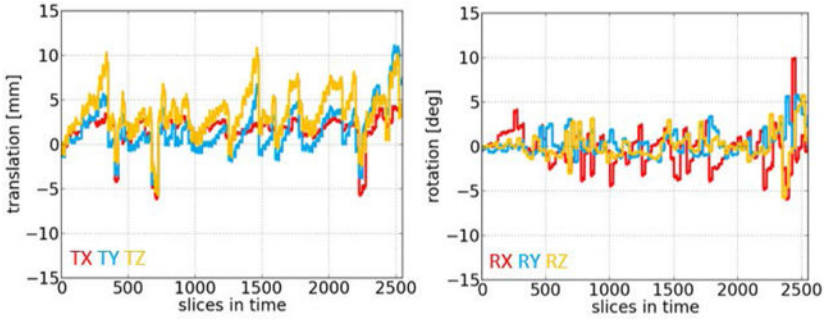

Figure 3.

Between-slice motion parameters (translation and rotation) measured and plotted for the consecutive slices (as acquired in time) of the T2*-w imaging sequence, for the example subject in 22GW.

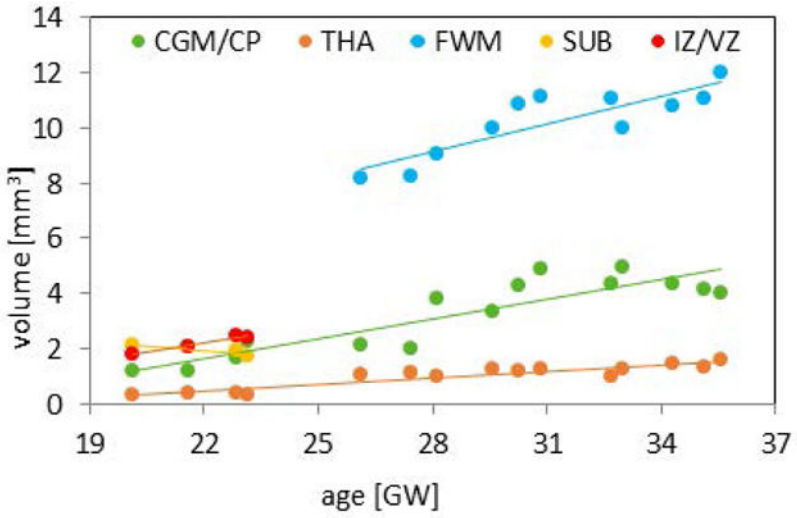

Figure 4.
The volumes of manually outlined ROIs for CGM/CP, THA, WM, SUB and IZ/VZ plotted against subjects' age.

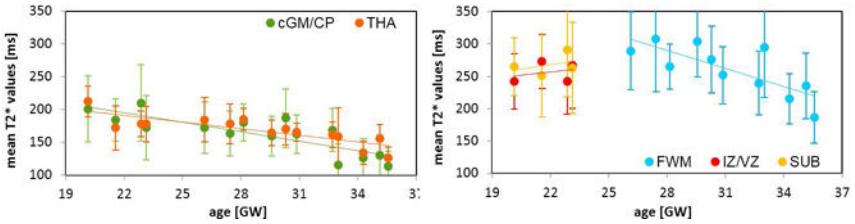

Figure 5.

Mean T2* values calculated within the ROIs for FWM, SUB, IZ/VZ, CGM/CP and THA plotted against the subjects' age with standard deviations marked by the error bars for each subject; decrease of CGM/CP and THA T2* values as well as FWM values significantly correlated with the increasing fetal age ($p<0.0001$ for CGM/CP and THA, $p<0.01$ for FWM).

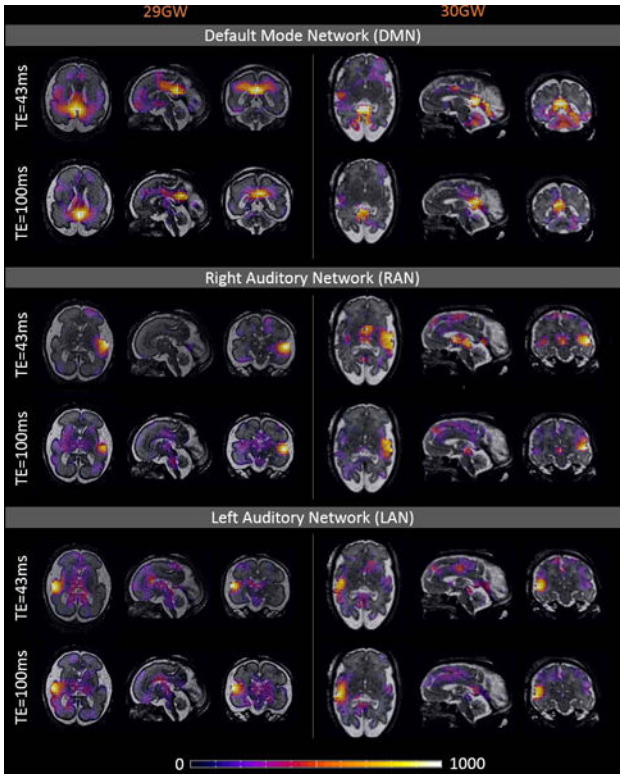

Figure 6.

Correlation maps calculated for seeds placed in praecuneus, right and left auditory cortex, for R2* maps obtained from the datasets including images acquired with 43ms and 100ms echo time, overlaid on the structural data. For both subjects (29 and 32GW) default mode network (DMN), right and left auditory network (RAN and LAN) appear to be better localized and less noisy in the maps obtained for the dataset with TE=100 ms.

Table 1

Comparison of the mean T2* values [ms] calculated within the ROIs for FWM, SUB, IZ/VZ, CGM/CP averaged across all the subjects with the previous results reported in the literature for fetal, newborn, infant and adults subjects.

subject	CGM/CP	THA	FWM/IZ&VZ	SUB	N	age	reference
fetus	**163±30**	**168±21**	**259±34**	**268±17**	**14** **3**	**29±5 GW** **22±1 GW**	**this study**
		154±24	234±38		15	32±3 GW	Vasylechko et al. 2014
newborn		155±48	180±38		4	33±1 W	Rivikin et al. 2004
		151±36	152±51		10	42±1 W	
infant		82±13	96±14		5	9 M	
adult		69±7	67±4		7	38±9 Y	
	84±1		66±2		6	37±11 Y	Peters et al. 2007

Mean T2* values within ROIs

Table 2

A summary of the percentage of brain voxels presenting a correlation above threshold 400 for two subjects and three seeds: default mode network (DMN), left and right auditory network (ANL and ANR).

subject	seed	TE=43 ms	TE=100 ms
subject 1	DMN	10.2	1.4
	ANL	3.4	2.1
	ANR	5.1	2.2
subject 2	DMN	6.2	2.4
	ANL	1.6	1.8
	ANR	2.2	1.0

Percentage of brain voxels presenting a correlation above threshold of 400.